



You have downloaded a document from  
**RE-BUŚ**  
repository of the University of Silesia in Katowice

**Title:** Neutrinos in proto-neutron star models

**Author:** Monika Pieńkos

**Citation style:** Pieńkos Monika. (2013). Neutrinos in proto-neutron star models. "Acta Physica Polonica B" (Vol. 44, no. 11 (2013), s. 2389-2395), doi 10.5506/APhysPolB.44.2389



Uznanie autorstwa - Licencja ta pozwala na kopiowanie, zmienianie, rozprowadzanie, przedstawianie i wykonywanie utworu jedynie pod warunkiem oznaczenia autorstwa.



UNIWERSYTET ŚLĄSKI  
W KATOWICACH



Biblioteka  
Uniwersytetu Śląskiego



Ministerstwo Nauki  
i Szkolnictwa Wyższego

## NEUTRINOS IN PROTO-NEUTRON STAR MODELS\*

MONIKA PIEŃKOS

Institute of Physics, University of Silesia  
Uniwersytecka 4, 40-007 Katowice, Poland

*(Received October 29, 2013)*

The equation of state (EoS) of a hot proto-neutron star matter with trapped neutrinos was calculated within the effective SU(3) theory with the enhanced vector meson sector.

DOI:10.5506/APhysPolB.44.2389

PACS numbers: 97.60.Jd, 26.60.Kp

## 1. Introduction

A scenario that was adopted to describe an evolution of a neutron star predicts that the formation of a cold catalysed object is preceded by very specific phases that define a proto-neutron star. The loss of lepton number from the collapsed star proceeds in separate stages. First, the deleptonization of the surface layer takes place in a very short time in comparison with the Kelvin–Helmholtz neutrino cooling time. After that, the deleptonization of the core proceeds by the emission of electron neutrinos which are produced efficiently via the  $\beta$ -processes. The initial moment  $t = 0$  characterizes the stage with neutrinos trapped ( $Y_L = 0.4$ ) both in the core and in the outer envelope. The deleptonization leads to a substantial reduction in the extension of the proto-neutron star envelope. The analysis of the evolutionary path of a proto-neutron star that leads to the formation of a cold neutron star with the masses in excess of two solar mass is of special importance in connection with the discovery of the binary millisecond pulsar J1614-2230 [1]. Construction of neutron star models with nonzero strangeness which result in a maximum mass exceeding two solar masses can also be done using models that involve deconfined phase of dense matter [2].

---

\* Presented at the XXXVII International Conference of Theoretical Physics “Matter to the Deepest” Ustroń, Poland, September 1–6, 2013.

## 2. The model

### 2.1. The equation of state

The presented model of a nascent neutron star is constructed on the basis of the hadronic SU(3) theory, which naturally includes nonlinear scalar and vector interaction terms. It is an effective model constructed within the framework of the nonlinear realization of the chiral SU(3)<sub>L</sub> × SU(3)<sub>R</sub> symmetry. Details can be found in the papers by Papazoglou *et al.* [3, 4]. A detailed description of the model that was used in this paper is given in [5, 6]. The characteristic feature of this model is the extended vector meson sector, that comprises different mixed vector meson couplings. This permits more accurate description of asymmetric strangeness-rich neutron star matter [5]. The Lagrangian function of the model takes the form

$$\begin{aligned} \mathcal{L} = & \sum_B \bar{\psi}_B (\gamma^\mu i D_\mu - m_{\text{eff},B}) \psi_B + \frac{1}{2} \partial^\mu \sigma \partial_\mu \sigma - \frac{1}{2} m_\sigma^2 \sigma^2 - \frac{1}{3} g_3 \sigma^3 - \frac{1}{4} g_4 \sigma^4 \\ & + \frac{1}{2} \partial^\mu \sigma^* \partial_\mu \sigma^* - \frac{1}{2} m_{\sigma^*}^2 \sigma^{*2} - \frac{1}{4} \Omega^{\mu\nu} \Omega_{\mu\nu} - \frac{1}{4} \mathbf{R}^{\mu\nu} \mathbf{R}_{\mu\nu} - \frac{1}{4} \Phi^{\mu\nu} \Phi_{\mu\nu} \\ & + \frac{1}{2} m_\omega^2 (\omega^\mu \omega_\mu) + \frac{1}{2} m_\rho^2 (\rho^{\mu a} \rho_\mu^a) + \frac{1}{2} m_\phi^2 (\phi^\mu \phi_\mu) + U_V(\omega, \rho, \phi) + \mathcal{L}_l, \end{aligned} \quad (1)$$

where  $\Omega_{\mu\nu}$ ,  $\mathbf{R}_{\mu\nu}$ , and  $\Phi_{\mu\nu}$  are the field tensors of the  $\omega$ ,  $\rho$ , and  $\phi$  mesons, and  $m_{\text{eff},B} = m_B - g_{N\sigma}\sigma - g_{N\sigma^*}\sigma^*$  denotes baryon effective mass.

The Lagrangian function (1) describes the  $\beta$ -equilibrated neutron star matter, thus there is also a need to consider the Lagrangian of free leptons  $\mathcal{L}_l = \sum_{l=e,\mu,\nu} \bar{\psi}_l (i\gamma^\mu \partial_\mu - m_l) \psi_l$ . The vector meson couplings are collected in the form of a vector meson potential

$$\begin{aligned} U^V(\omega, \rho, \phi) = & \frac{1}{4} c_3 (\omega^\mu \omega_\mu)^2 + \frac{1}{4} c_3 (\rho^{\mu a} \rho_\mu^a)^2 + \frac{1}{8} c_3 (\phi^\mu \phi_\mu)^2 \\ & + A_V (g_{N\omega} g_{N\rho})^2 (\omega^\mu \omega_\mu) (\rho^{\mu a} \rho_\mu^a) + \frac{1}{4} A_V (g_{N\omega} g_{N\rho})^2 (\phi^\mu \phi_\mu)^2 \\ & + \frac{1}{2} \left( \frac{3}{2} c_3 - A_V (g_{N\omega} g_{N\rho})^2 \right) (\phi^\mu \phi_\mu) (\omega^\mu \omega_\mu + \rho^{\mu a} \rho_\mu^a). \end{aligned} \quad (2)$$

When the considered model takes into account only nucleons, the vector meson potential  $U_{S \neq 0}^V$  is reduced to a very simple form

$$U_{S \neq 0}^V = \frac{1}{4} c_3 (\omega^\mu \omega_\mu)^2 + A_V (g_{N\omega} g_{N\rho})^2 (\omega^\mu \omega_\mu) (\rho^{\mu a} \rho_\mu^a). \quad (3)$$

The composition of the matter of a proto-neutron star is determined by the requirements of charge neutrality and generalized  $\beta$  equilibrium. Calculations of the equation of state have been done in the mean field approach. In this approximation, meson fields are separated into classical mean field

values:  $s_0, s_0^*, w_0, r_0, f_0$  and quantum fluctuations, which are neglected in the ground state. The pressure of the matter of a proto-neutron star was calculated from the energy momentum tensor and takes a form

$$\begin{aligned}
 P = & -\frac{1}{2}m_\sigma^2 s_0^2 - \frac{1}{3}g_3 s_0^3 - \frac{1}{4}g_4 s_0^4 - \frac{1}{2}m_{\sigma^*}^2 s_0^{*2} + \frac{1}{2}m_\omega^2 w_0^2 + \frac{1}{2}m_\rho^2 r_0^2 + \frac{1}{2}m_\phi^2 f_0^2 \\
 & + \frac{1}{4}c_3 (w_0^4 + r_0^4) + \Lambda_V (g_{N\omega} g_{N\rho})^2 w_0^2 r_0^2 + \left( \frac{1}{8}c_3 + \frac{1}{4}\Lambda_V (g_{N\omega} g_{N\rho})^2 \right) f_0^4 \\
 & + \left( \frac{3}{4}c_3 - \frac{1}{2}\Lambda_V (g_{N\omega} g_{N\rho})^2 \right) f_0^2 (w_0^2 + r_0^2) \\
 & + \sum_{i=B,l} \left\{ \frac{2J_i + 1}{3(2\pi)^3} \int d^3k \frac{k^2}{\sqrt{k^2 + m_{\text{eff},i}^2}} (f_i^+(k) + f_i^-(k)) \right\}, \tag{4}
 \end{aligned}$$

where  $f_i^+$  and  $f_i^-$  are Fermi functions respectively for particles and antiparticles, and  $J_i$  denotes the spin.

### 2.2. Coupling constants

The potential that describes hyperon–nucleon (YN) and hyperon–hyperon (YY) interactions can be written in the form  $U_Y^{(B)} = g_{Y\sigma} s_0 - g_{Y\omega} w_0 + g_{Y\sigma^*} s_0^* - g_{Y\phi} f_0$ , which allows one to determine the scalar coupling constants. The  $g_{Y\sigma}$  coupling constants were obtained for the following values of the potentials:  $U_\Lambda^{(N)} = -28$  MeV,  $U_\Sigma^{(N)} = 30$  MeV,  $U_\Xi^{(N)} = -18$  MeV, while the couplings of hyperons to the strange meson  $\sigma^*$  were calculated from relations:  $U_\Xi^{(\Xi)} \simeq U_\Lambda^{(\Xi)} \simeq 2U_\Xi^{(\Lambda)} \simeq 2U_\Lambda^{(\Lambda)}$ . The  $\Lambda_V$  parameter describes the strength of the  $\omega$ – $\rho$  coupling and requires the adjustment of the  $g_{N\rho}$  coupling constant to keep the empirical value of the symmetry energy  $E_{\text{sym}}(n_b) = 25.68$  MeV at the baryon density  $n_b$ , which corresponds to  $k_F = 1.15 \text{ fm}^{-1}$  [7]. The coupling constants are collected in Table I.

TABLE I

The coupling constants.

$g_{\Lambda\sigma}$	$g_{\Xi\sigma}$	$g_{\Sigma\sigma}$	$g_{\Lambda\sigma^*}$	$g_{\Xi\sigma^*}$	$g_{\Sigma\sigma^*}$	$\frac{g_{N\rho}}{\Lambda_V = 0}$	$\frac{g_{N\rho}}{\Lambda_V = 0.0165}$
6.169	3.201	4.476	5.262	11.623	5.626	9.264	10.037

### 3. Results and conclusions

The analysis of proto-neutron star models with conserved electron lepton number was done on the basis of the TM1-nonlinear model. The obtained forms of the EoSs are plotted in Fig. 1 (a). When hyperons are included, calculations have been done for the model (TM1-weak) which includes only  $\omega$ - $\rho$  coupling ( $\phi$  and  $\sigma^*$  mesons introduced in a minimal fashion [8, 9]) and the one (EXT) that embodies a broad spectrum of nonlinear vector meson interactions presented in equation (2). Analysis of the results obtained for the matter of proto-neutron stars with nonzero strangeness indicates a clear stiffening of the EoS in the case of nonlinear model. Calculations were done for the chosen value of parameter  $\Lambda_V = 0.0165$ . After obtaining the EoS, the mass and radius of a star were calculated for a given value of the central density. This can be done by integrating the Tolman–Oppenheimer–Volkoff equations. The resulting mass–radius relations are presented in Fig. 1 (b). Comparing the results obtained for the minimal TM1-weak model and the extended TM1 nonlinear model, a significant increase in mass of the star is evident. This figure comprises also mass–radius relations obtained in the case of nuclear matter.

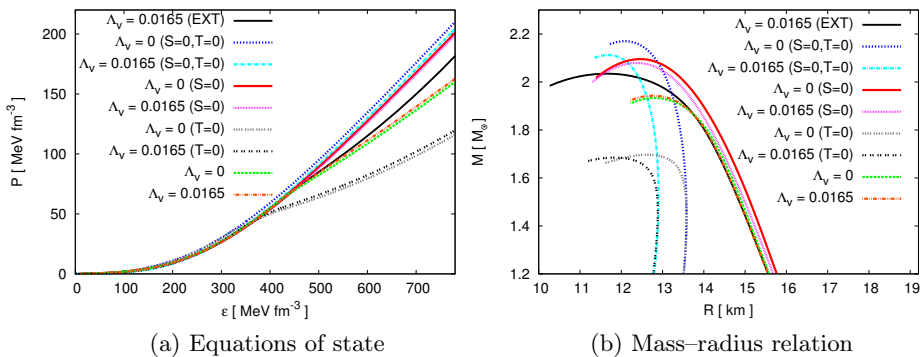


Fig. 1. EoSs and mass–radius relations calculated for a warm proto-neutron star matter with trapped neutrinos and for a cold neutrino-free matter ( $T = 0$ ), in the case of nuclear matter ( $S = 0$ ) and in the case of hyperon-rich matter. Calculations have been done for different values of  $\Lambda_V$  parameter. For comparison, results for the extended model (EXT) are included.

The main objective of this paper was to investigate the effect of neutrinos on the structure and properties of a proto-neutron star. Our analysis concerns the abundance of neutrinos and their energy in neutron star interiors (Fig 2). The results obtained in the case of the extended, nonlinear model with nonzero strangeness resemble that of nuclear matter. In this paper, the internal structure of a proto-neutron star was examined. The inner core of a neutron star in the case of hyperon rich matter comprises a hyperon core.

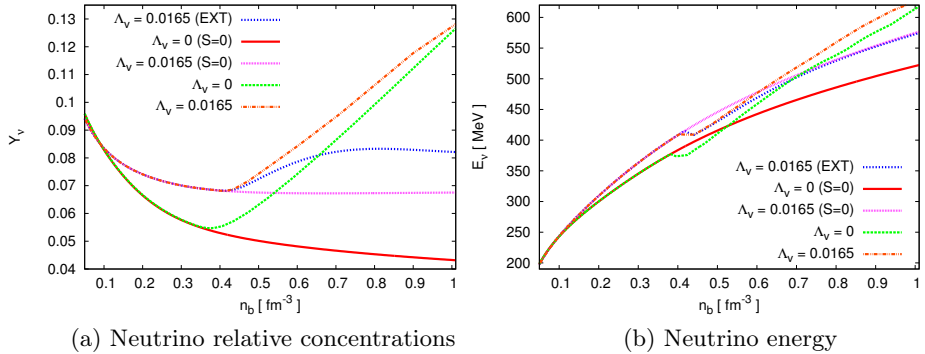


Fig. 2. Relative concentrations of neutrinos and neutrino energy as a function of baryon number density obtained for different values of  $\Lambda_V$  parameter in the case of nonstrange and strangeness-rich matter.

Table II compiles the results of numerical calculations for the hyperon core performed for both the TM1-weak model and the nonlinear extended model. Both the proto-neutron star and cold, deleptonized neutron star model with the extended vector meson sector result in a hyperon core with a much larger mass and radius. The onset points for hyperons were left almost unchanged. Calculations were done for the maximum mass configurations.

TABLE II

Mass and radius of hyperon core, as well as baryon density of the first hyperon onset point, obtained for the considered models of hyperon stars.

$\Lambda_V$	$T = 0$			$T \neq 0$		
	$M_{hc}$ [ $M_\odot$ ]	$R_{hc}$ [km]	$n_{b,\text{onset}}$ [fm <sup>-3</sup> ]	$M_{hc}$ [ $M_\odot$ ]	$R_{hc}$ [km]	$n_{b,\text{onset}}$ [fm <sup>-3</sup> ]
0	0.723	7.366	0.316	0.862	7.195	0.391
0.0165	0.809	7.288	0.346	0.789	6.891	0.416
0.0165 (EXT)	1.617	8.309	0.348	1.244	7.579	0.416

The sensitivity of the calculations to different nonlinear vector meson couplings is also indicated in the analysis of radial dependence of neutrino concentrations and neutrino energies for the maximum mass configurations (Fig. 3). The largest difference occurs in the case of neutrino concentrations. The extended nonlinear model considerably reduced neutrino concentration in the very inner part of the hyperon core. The most significant result was obtained for the radial dependence of the pressure (Fig. 4). In the case of the extended model, the pressure in the inner part of the hyperon core is much higher than the one calculated for the TM1-weak model.

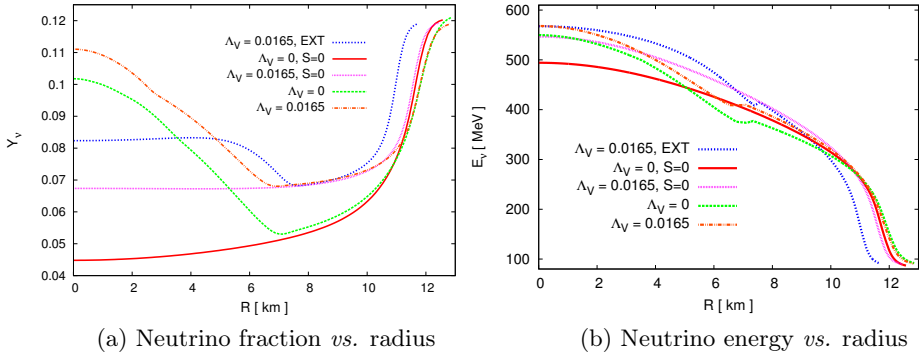


Fig. 3. Results obtained for maximum mass configurations for different values of  $\Lambda_V$  parameter in the case of nonstrange and strangeness-rich matter.

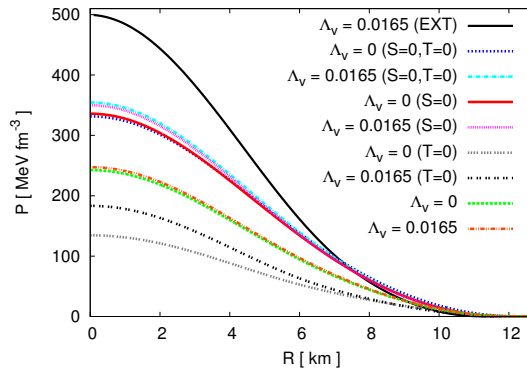


Fig. 4. Pressure vs. neutron star radius obtained for maximum mass configurations for different values of  $\Lambda_V$  parameter. Calculations have been done for warm neutrino-rich and cold neutrino-free matter in the case of a nonstrange neutron star as well as a hyperon star.

In summary, the presence of nonlinear vector meson couplings leads to important changes in proto-neutron star parameters and structure leading to a considerable increase of proto-neutron star mass. Another effect connected with the use of the extended model is the reduced concentrations of neutrinos in the hyperon core. The hyperon core itself was also altered by the nonlinear vector meson couplings that lead to the increase of the hyperon core mass.

## REFERENCES

- [1] P. Demorest *et al.*, *Nature* **467**, 1081 (2010).
- [2] R. Manka, I. Bednarek, G. Przybyla, *New J. Phys.* **4**, 14 (2002).
- [3] P. Papazoglou *et al.*, *Phys. Rev.* **C57**, 2576 (1998).
- [4] P. Papazoglou *et al.*, *Phys. Rev.* **C59**, 411 (1999).
- [5] I. Bednarek *et al.*, *Astron. Astrophys.* **543**, A157 (2012).
- [6] I. Bednarek, R. Manka, *J. Phys. G* **36**, 095201 (2009).
- [7] C.J. Horowitz, J. Piekarewicz, *Phys. Rev. Lett.* **86**, 5647 (2001).
- [8] I. Bednarek, R. Manka, *Phys. Rev.* **C73**, 045804 (2006).
- [9] I. Bednarek, M. Pieńkos, *Acta Phys. Pol. B* **42**, 2221 (2011).